Journal of Organometallic Chemistry, 389 (1990) 301–313
Elsevier Sequoia S.A., Lausanne – Printed in The Netherlands
JOM 20773

An electron spin resonance study of the 2,5-diphenylchalcophene radical ions

Alwyn G. Davies and Carl H. Schiesser

Chemistry Department, University College London, 20 Gordon Street, London WC1H 0AJ (United Kingdom)

(Received January 4th, 1990)

Abstract

The 2,5-diphenylchalcophene radical ions (chalcogen = O, S, Se, Te) have been prepared by the action of alkali metal in 1,2-dimethoxyethane (anions), or by the action of sulphuric acid or thallium(III) trifluoroacetate in trifluoroacetic acid (TFAH) (cations), on the parent compounds. The ESR spectra of these radical ions have been interpreted as belonging to systems which are conformationally rigid on the ESR timescale, as is evident from the non-equivalence of the *ortho*- and *meta*-proton hyperfine coupling constants.

The furan, thiophene and selenophene radical ions exhibit ESR spectra which are consistent with the expectation that the LUMO of the parent is symmetric and the HOMO, antisymmetric. The tellurophene radical anion shows a coupling to ^{125}Te of 13.5 G in its ESR spectrum, while the spectrum of the tellurophene radical cation suggests that a change in the nature of the HOMO might have occurred in progressing down the series.

When the tellurophene was photolysed in H_2SO_4/TFAH, the ESR spectrum of the furan radical cation was observed. The implication of this is discussed.

Introduction

Electron spin resonance (ESR) spectroscopy provides a powerful method of probing the spatial properties of semi-occupied molecular orbitals. ESR techniques can yield information about the LUMO of a molecule through reduction to the radical anion with alkali metals, resulting in population of the lowest unoccupied molecular orbital (LUMO) of the parent molecule with a single electron. Analysis of the hyperfine coupling constants between the unpaired electron and magnetically active nuclei in the molecule provides data concerning electron distribution in the LUMO.

0022-328X/90/$03.50 © 1990 – Elsevier Sequoia S.A.

1

2 (ψ_A)

3

4 (ψ_s)

5 (ψ_s)

6

In similar fashion, established techniques [1–6] can probe the highest occupied molecular orbital (HOMO) through formation of the radical cation. Even so, few examples of the ESR spectra of radical ions of heterocyclic systems have been reported [7–10].

In order to rectify this anomaly, we have recently reported [9] an ESR study of the radical cations of some substituted pyrroles, furans and thiophenes (**1**, X = NR, O, S) in fluid solution. This study, together with those of other workers [7,8], has supported the expectation that the HOMO in these heterocyclic systems (**1**) is antisymmetric (ψ_A) and similar to **2**.

The radical cations of **1** are π-isoelectronic with the cyclopentadienyl radical (**3**) in which ψ_A is one of a degenerate pair, the other orbital being symmetric (ψ_S) and similar to **4**. This degeneracy is broken when **3** is substituted, or when a heteroatom is introduced into the ring.

The chalcophenes (**1**, X = O/S/Se/Te) are a series of heterocycles in which the heteroatom becomes more electropositive as the atomic number increases in progressing down Group IV. In furan, the heteroatom is expected to stabilize ψ_S and in doing so to perturb the orbital itself so that **5** becomes a better representation of ψ_S [11]. In thiophene, selenophene and tellurophene, this stabilizing effect is less obvious. Calculations [11] suggest that while ψ_S is less stabilized when X = S and even less so when X = Se, ψ_A still remains the HOMO. These calculations also suggest that the LUMO remains relatively unchanged throughout the series, resembling **6**.

When X = Te, however, these same calculations propose that the symmetrical orbital (**5**) is the HOMO, presumably because the electropositive nature of tellurium destabilizes ψ_A relative to ψ_S. A low-lying σ^* anti-bonding orbital is predicted to be of similar energy to the LUMO, **6**.

While the spatial properties of these orbitals are unlikely to be affected by substitution on the heterocyclic ring (**1**), their relative ordering might, as alkyl substituents in the 2 and 5 positions of **1** will be expected to destabilize ψ_A over ψ_S through a hyperconjugative mechanism. This effect might be great enough to overcome the electropositive destabilization of ψ_S by tellurium.

Work in our laboratories has shown [9] that the radical cations of **1** (X = NR/S/O) in fluid solution give rise to spectra which are not consistent with $\mathbf{1}^{\ddagger}$. We have attributed this to rapid polymerization of the radical cations through the 2 and

5 positions, where the coefficients of ψ_A are largest. This problem is overcome when **1** is 2,5-disubstituted.

With this in mind, we now report a systematic ESR study of the radical ions of the 2,5-diphenylchalcophenes (**7**), which are readily prepared disubstituted systems with the advantage of forming extensively conjugated and stabilized radical ions.

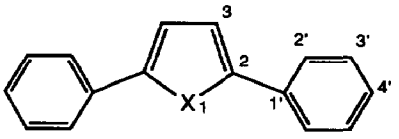

7a : X = O
b : X = S
c : X = Se
d : X = Te

Results

A. Radical anions

The radical anions of the 2,5-diphenylchalcophenes, (**7a**–**7c**$^{\cdot-}$) were conveniently prepared by treating a solution of **7a**–**7c** in dry 1,2-dimethoxyethane (DME) with freshly distilled potassium metal and are pink in colour. The ESR spectra of the furan radical anion (**7a**$^{\cdot-}$) and the thiophene radical anion (**7b**$^{\cdot-}$) are identical with those previously reported [12,13]. Our assignment of the hyperfine coupling constants in **7a**,**7b**$^{\cdot-}$, and, indeed, in the remaining radical anions in the series (**7c**,**7d**$^{\cdot-}$) is based on these previous reports, our INDO hyperfine coupling calculations [14] for **7a**$^{\cdot-}$ and the trends apparent in the series.

The technique described as above, when applied to the tellurophene (**7d**), resulted in a green solution with no corresponding ESR spectrum. Presumably **7d** is being over-reduced by the action of potassium, to form the magnetically inactive dianion (**7d**$^{2-}$).

In order to overcome this problem, we attempted to generate **7d**$^{\cdot-}$ through the use of sodium metal. This method was unsuccessful even after the solution, in contact with the metal, was sonicated for 8 h. When this experiment was repeated, however, using sodium and DME in conjunction with crown ether (18-crown-6), an intense purple solution was rapidly formed, which exhibited the ESR spectrum shown in Fig. 1. The winglines of this spectrum could only be successfully simulated (Fig. 1) when ^{125}Te satellites at 7% abundance were incorporated into the simulation *. This yielded a hyperfine coupling to ^{125}Te of 13.5 G.

The spectroscopic data pertaining to the radical anions (**7**$^{\cdot-}$) are listed in Table 1, together with INDO results for **7a**$^{\cdot-}$. The ESR spectrum of the selenophene radical anion (**7c**$^{\cdot-}$) is shown in Fig. 2, together with the computer simulation.

* Tellurium has only two magnetically active nuclei of any significance: ^{125}Te ($I = \frac{1}{2}$, 6.99%) and ^{123}Te ($I = \frac{1}{2}$, 0.9%).

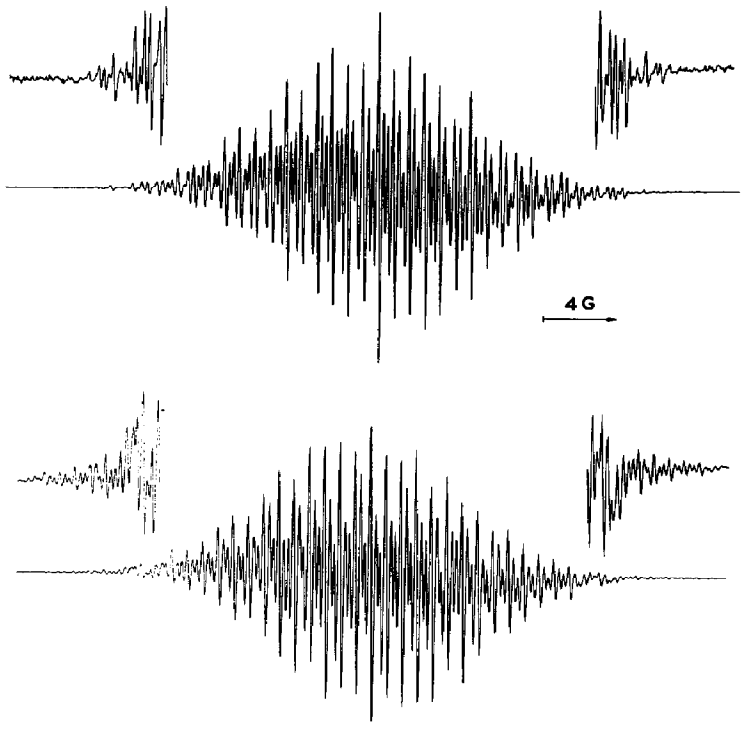

Fig. 1. The ESR spectrum of the 2,5-diphenyltellurophene radical anion ($7d^{\cdot-}$) in DME at $-30\,^{\circ}C$ (above) and computer simulation (below).

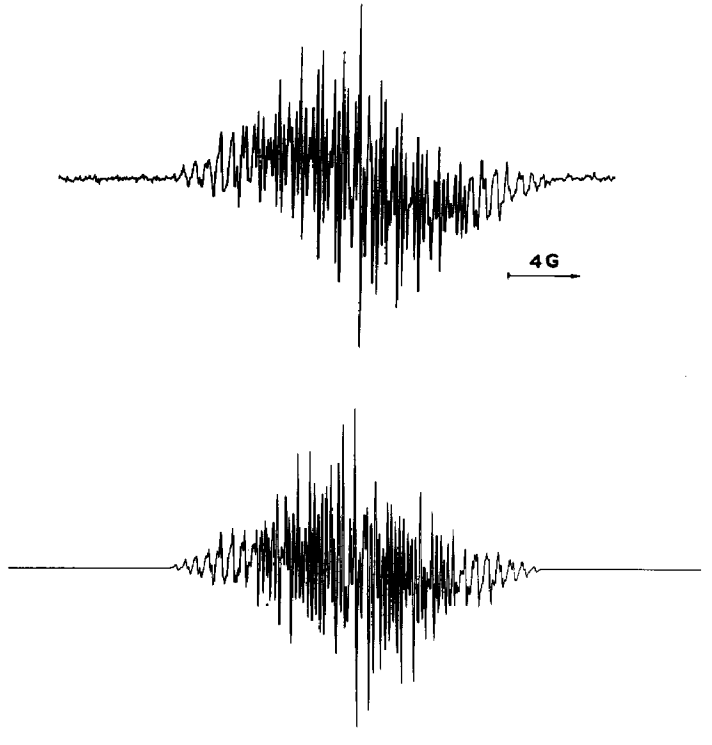

Fig. 2. The ESR spectrum of the 2,5-diphenylselenophene radical anion ($7c^{\cdot-}$) in DME at $-43\,^{\circ}C$ (above) and computer simulation (below).

B. Radical cations

When the 2,5-diphenylchalcophenes (**7a–7c**) were dissolved in trifluoroacetic acid (TFAH), they exhibited very weak ESR spectra in the absence of photolysis. We have interpreted these spectra as corresponding to the radical cations (**7a–7c**$^{\ddagger+}$). When concentrated sulphuric acid (H_2SO_4) (ca. 5%) was added, the spectra showed a marked increase in intensity and these conditions (5% H_2SO_4/TFAH) were chosen as standard in the preparation of these radical cations.

The ESR spectra of **7a–7c**$^{\ddagger+}$ and their computer simulations are displayed in Fig. 3–5, while the spectroscopic data are listed in Table 2. Assignment of proton-hyperfine coupling constants in these cations is based on INDO calculations performed on the furan radical cation (**7a**$^{\ddagger+}$) and trends apparent throughout the series and are tentative, due to several similar couplings in each case. These INDO data are included in Table 2.

When the tellurophene (**7d**) was dissolved in the acidic mixture (5% H_2SO_4/TFAH) as previously described, no ESR spectrum was observed. Photolysis with light from a high-pressure mercury arc filtered through Pyrex glass, as had been necessary in other cases [9], resulted in a spectrum, which persisted after photolysis and was identical to that of the furan radical cation (**7a**$^{\ddagger+}$). A precipitate of tellurium was also noticed. The implications of this observation will be discussed later.

In order to overcome what appears to be the formation of the furan radical cation (**7a**$^{\ddagger+}$), we chose to use mercury(II) trifluoroacetate or thallium(III) trifluoroacetate in TFAH, as described by Kochi [2–6]. The mercury salt was unsuccessful, but, when **7d**, dissolved in TFAH containing thallium(III) trifluoroacetate was

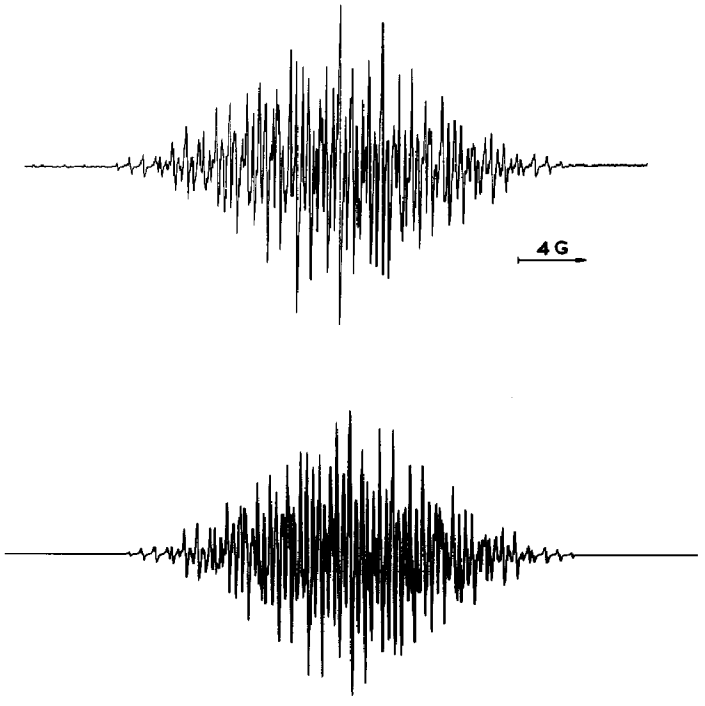

Fig. 3. The ESR spectrum of the 2,5-diphenylfuran radical cation (**7a**$^{\ddagger+}$) in 5% H_2SO_4/TFAH at −15 °C (above) and computer simulation (below).

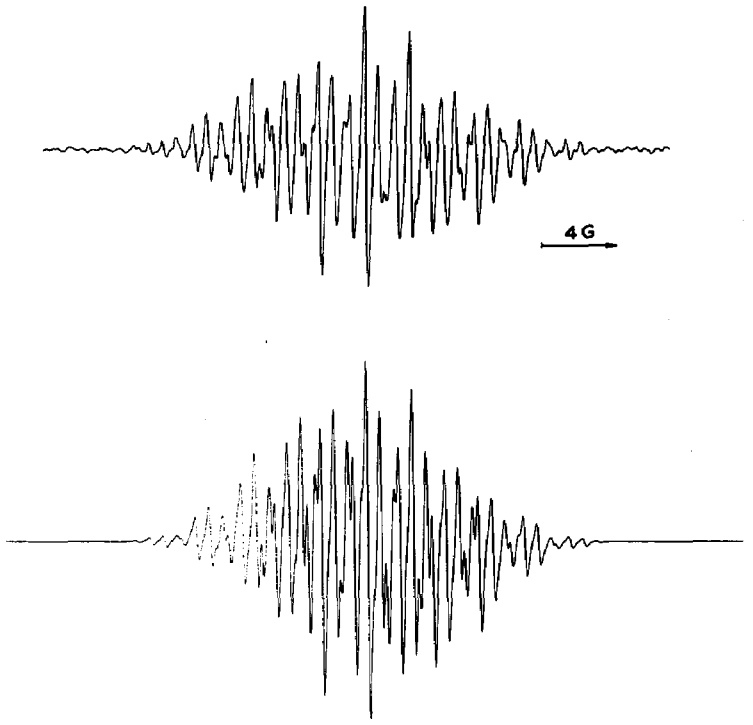

Fig. 4. The ESR spectrum of the 2,5-diphenylthiophene radical cation ($7b^{+\cdot}$) in 5% H_2SO_4/TFAH at −15 °C (above) and computer simulation (below).

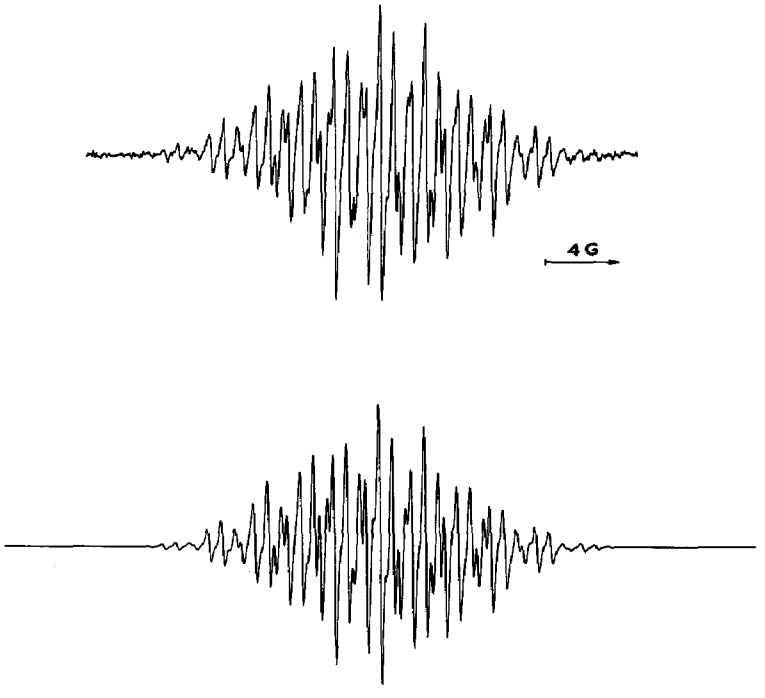

Fig. 5. The ESR spectrum of the 2,5-diphenylselenophene radical cation ($7c^{+\cdot}$) in 5% H_2SO_4/TFAH at −15 °C (above) and computer simulation (below).

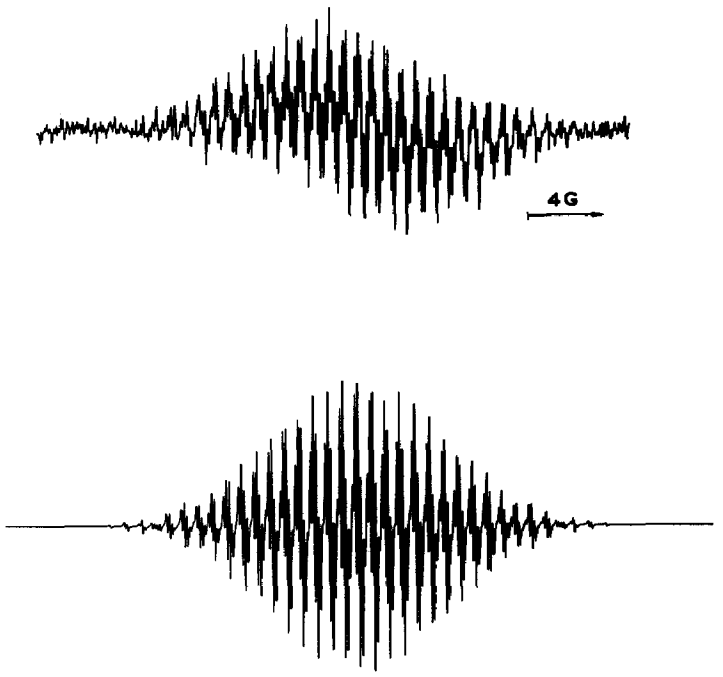

Fig. 6. The ESR spectrum of the 2,5-diphenyltellurophene radical cation ($7d^{+\cdot}$) generated by photolysis in TFAH containing thallium (III) trifluoroacetate at −15 °C (above) and computer simulation (below).

Table 1

ESR spectral parameters [a] of 2,5-diphenylchalcophene radical anions ($7^{-\cdot}$) in 1,2-dimethoxyethane

Radical anion	Hyperfine coupling constants (G)					
	H-3	H-2′	H-3′	H-4′	X	g
$7a^{-\cdot}$	0.80(0.49)	2.00(3.04)	0.40(1.63)	3.81(3.55)	–	2.0025
		2.41(3.06)	0.60(1.63)			
$7b^{-\cdot}$	1.20	1.85	0.42	3.13	–	2.0036
		2.26	0.62			
$7c^{-\cdot}$	1.29	1.95	0.50	3.07	–	2.0064
		2.20	0.63			
$7d^{-\cdot}$	1.61	2.42	0.31	4.82	13.5	2.0027
		3.18	0.51			

[a] INDO results in parentheses

Table 2

ESR spectra parameters [a] of 2,5-diphenylchalcophene radical cations ($7^{+\cdot}$) in trifluoroacetic acid

Radical cation	Hyperfine coupling constants (G)				
	H-3	H-2′	H-3′	H-4′	g
$7a^{+\cdot}$	2.78 [b](2.51)	2.41 [b](2.57)	0.69(1.39)	3.38(2.72)	2.0025
		2.42 [b](2.60)	0.77(1.41)		
$7b^{+\cdot}$	2.48 [b]	2.42 [b]	0.73	3.48	2.0023
$7c^{+\cdot}$	2.40 [b]	2.38 [b]	0.73	3.40	2.0007
$7d^{+\cdot}$	2.99 [b]	2.22 [b]	0.78	3.80 [b]	2.0025
		2.37 [b]	0.93		

[a] INDO results in parentheses. [b] these values are interchangeable (see text).

irradiated with unfiltered light from the mercury arc, the ESR spectrum shown in Fig. 6 was observed. Computer simulation yielded the hyperfine coupling constants displayed in Table 2. Assignment of these couplings is also tentative, especially at the heterocyclic (H-3) and *para* (H-4′) positions, because $\mathbf{7d}^{+}$ exhibits an ESR spectrum significantly different to the other 2,5-diphenylchalcophene radical cations.

Discussion

In their study of the 2,5-diphenylthiophene radical anion ($\mathbf{7b}^{\cdot-}$) and other substituted thiophenes, Pedulli and co-workers [12] noted that $\mathbf{7b}^{\cdot-}$ is conformationally rigid about the C-2–C-1′ bond on the ESR timescale, as is evident by the non-equivalence of the hyperfine coupling constants to the *ortho* (H-2′) and *meta* (H-3′) protons, even at 60 °C. Herold and co-workers [13] also observed similar non-equivalence in their study of 2,5-diarylfuran radical anions.

Inspection of Table 1 clearly reveals this non-equivalence in our study and indicates the generality of this conformational rigidity throughout the series, as the selenophene and tellurophene radical anions ($\mathbf{7c}^{\cdot-}$, $\mathbf{7d}^{\cdot-}$) also show non-equivalent couplings to their *ortho*- and *meta*-protons.

Table 2 also indicates the rigidity associated with the 2,5-diphenylfuran radical cation ($\mathbf{7a}^{\cdot+}$) and that of the tellurophene ($\mathbf{7d}^{\cdot+}$). In the case of the thiophene and selenophene radical cations ($\mathbf{7b}^{\cdot+}$, $\mathbf{7c}^{\cdot+}$), no inequivalence in the hyperfine coupling constants to *ortho*- and *meta*-protons could be detected. We could not determine whether or not the inequivalence lies buried in the increased linewidth associated with the ESR spectra of these cations (see Fig. 4 and 5).

In order to shed further light on this subject, we have determined the rotational barriers associated with the furan (**7a**) and its radical ions ($\mathbf{7a}^{\cdot+}$, $\mathbf{7a}^{\cdot-}$) using semi-empirical molecular orbital theory. PM3 calculations [15,16] suggest that the barriers to rotation about the C-2–C-1′ bond in **7a**, $\mathbf{7a}^{\cdot+}$ and $\mathbf{7a}^{\cdot-}$ are 1.3, 7.2 and 9.6 kcal mol^{-1} respectively. These results indicate that while the parent compound (**7a**) is essentially non-rigid on the ESR timescale, with freely rotating phenyl groups, both radical ions are expected to be held predominantly planar, with larger barriers to rotation.

Analysis of the molecular orbitals generated by PM3 indicates the origin of this relative rigidity. The HOMO and LUMO orbitals of **7a** are distributed according to **8** and **9**. Consequently, formation of the radical cation and the associated depopulation of the HOMO (**8**) reduces the π-antibonding interaction between C-2 and C-1′. Similarly, formation of the radical anion and population of the LUMO (**9**) increases bonding character between C-2 and C-1′. Thus, both anion and cation have an increased rotational barrier over that of the parent.

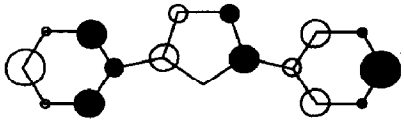

8 (HOMO)

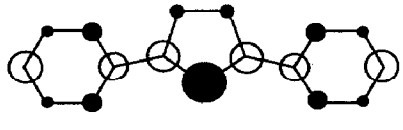

9 (LUMO)

The hyperfine coupling constants associated with the 2,5-diphenylchalcophene radical anions ($\mathbf{7}^{\cdot-}$) are consistent with a semi-occupied molecular orbital (SOMO)

distributed according to **9** in these systems. In progressing from the furan ($\mathbf{7a}^{\cdot-}$) to the thiophene, a slight decrease is observed in what we have identified to be the *ortho* (H-2′) hyperfine coupling constant. An increase of 0.4 G is observed for the coupling to the heterocyclic protons (H-3) and a decrease of 0.7 G is observed for the coupling to the *para* (H-4′) protons. The overall spectral width of 19.0 G for $\mathbf{7b}^{\cdot-}$ as compared with 20.0 G for $\mathbf{7a}^{\cdot-}$ indicates that some spin has shifted to the "hidden" centres, namely C-2 and C-1′ or the heteroatom in going from the furan to the thiophene.

This trend is further observed in progressing to the selenophene radical anion ($\mathbf{7c}^{\cdot-}$), in which coupling to what we have identified as the heterocyclic protons (H-3) is 1.29 G, while a further reduction at the *para* (H-4′), to a value of 3.07 G is noticed. The overall spectral width of 19.6 G indicates somewhat less spin at the "hidden" centres as compared with $\mathbf{7b}^{\cdot-}$.

The tellurophene radical anion ($\mathbf{7d}^{\cdot-}$), shows some interesting features in its ESR spectrum. The hyperfine coupling to what we believe are the heterocyclic protons (H-3) shows an increase to a value of 1.61 G. This is twice the coupling observed in the furan ($\mathbf{7a}^{\cdot-}$). Coupling to the *ortho* protons (H-2′) also increases, as does the coupling to the *para* proton, which exhibits the large value of 4.82 G. The overall spectral width is also significantly larger and at 25.7 G indicates a significant shift in spin density away from the "hidden" positions. The observed hyperfine coupling to ^{125}Te of 13.5 G is indicative of some spin on the heteroatom and also consistent with **9** as the SOMO. We are not aware of any other examples of the ESR spectroscopy of organotellurides.

The SOMO (**9**) involved in these systems will be expected to be affected by the nature of the chalcogen. When the heteroatom X is strongly electronegative, as it is in $\mathbf{7a}^{\cdot-}$, we might expect **9** to be stabilized, with a large coefficient on X. In the case of the thiophene ($\mathbf{7d}^{\cdot-}$) and selenophene ($\mathbf{7c}^{\cdot-}$), in which the heteroatom is less electronegative, one would expect **9** to be perturbed such that somewhat less coefficient would residue on the heteroatom. In the case of the tellurophene ($\mathbf{7d}^{\cdot-}$) with a strongly electropositive heteratom, we might expect the SOMO (**9**) to be perturbed such that significantly less spin density is located on the heteroatom, resulting in larger coefficients at the other positons in the molecule.

It is noteworthy that we were unable to detect a coupling to selenium in the spectrum of $\mathbf{7c}^{\cdot-}$. Selenium, like tellurium, has an abundance of magnetically inactive isotopes. Only ^{77}Se ($I = \frac{1}{2}$), with a natural abundance of 7.6% is active. We might, therefore, expect to observe ^{77}Se satellites in the spectrum of $\mathbf{7c}^{\cdot-}$. Inspection of Fig. 1 and 2 indicates that the ESR spectrum of the tellurophene radical anion ($\mathbf{7d}^{\cdot-}$) has a much better signal to noise ratio than that of the selenophene radical anion ($\mathbf{7c}^{\cdot-}$). It is possible, then, that the ^{77}Se satellites in Fig. 2 are lost in the noise, or even that the magnitude of the coupling is smaller, burying the satellites under the main spectrum.

It is also noteworthy that Herold et al. [13] reported slight changes in the hyperfine coupling constants associated with $\mathbf{7a}^{\cdot-}$ as the counterion was altered. As we are generating $\mathbf{7d}^{\cdot-}$ using sodium, we might expect slight differences in our ESR spectrum of $\mathbf{7d}^{\cdot-}$ when compared to the spectrum which might have been observed had we been successful with potassium. As the differences noted by Herold are small, together with the observation that sodium reduces the coupling to H-3 and increases the coupling to H-4′ in $\mathbf{7a}^{\cdot-}$ over potassium, we feel that our sodium-gen-

erated spectrum of $\mathbf{7d}^{\cdot-}$ will still provide a good qualitative picture of the trends operating in these radical anions.

The hyperfine coupling constants associated with the 2,5-diphenylfuran radical cation ($\mathbf{7a}^{+}$) (Table 2) are similar to the values calculated by INDO. As previously mentioned, these INDO calculations form the basis of our assignments in Table 2.

Inspection of Table 2 shows a smaller change in the hyperfine coupling constants to all protons in progressing from the furan ($\mathbf{7a}^{+}$) to the selenophene ($\mathbf{7c}^{+}$) than was previously noted for the analogous radical anions. The only noteable change is that of the coupling to what which we believe to be the heterocyclic protons (H-3), a decrease of 0.3G in $\mathbf{7b}^{+}$ over $\mathbf{7a}^{+}$.

Once again, large increases are observed for most couplings in the tellurophene radical cation ($\mathbf{7d}^{+}$). We feel that if the SOMO in ($\mathbf{7d}^{+}$) were similar to **8**, then the heteroatom would be expected to have only a small effect on the spin distribution, as it lies in the nodal plane of **8**. As the tellurium is having a noticeable effect, the HOMO associated with **7d** might indeed not reflect ψ_A, but in fact be better represented by a HOMO which is more ψ_S-like in the heterocyclic portion. This orbital would have a sizeable coefficient on tellurium and therefore be subject to the same electronic push associated with $\mathbf{7d}^{\cdot-}$. Of course, one would expect to observe some coupling to ^{125}Te. This hyperfine coupling, if present, could easily be lost in the noise present in the spectrum of $\mathbf{7d}^{+}$ (Fig. 6).

The *g*-values observed in the radical ions of **7** display the usual distribution seen in similar systems. Thus, the value of 2.0025 for both radical ions of **7a** is similar to the 2.0021–2.0023 reported for other furan radical cations [9]. The value of 2.0023 for $\mathbf{7b}^{+}$ is also within the range reported for the thiophene radical cations (2.0019–2.0027) [9]. The value of 2.0036 for $\mathbf{7b}^{\cdot-}$ shows a similar increase in *g*-value to other systems with sizeable coefficient on the heteroatom [17], as does the value of 2.0064 for $\mathbf{7c}^{\cdot-}$. The *g*-value of the selenophene radical cation ($\mathbf{7c}^{+}$), at 2.0007 is identical with that of the radical cation of tetramethylselenophene [18].

We have no ESR spectra of other organotellurium systems with which to compare the *g*-values for $\mathbf{7d}^{\cdot-}$ and $\mathbf{7d}^{+}$. The values of 2.0027 for the anion and 2.0025 for the cation are remarkably different from the selenophene radical ions ($\mathbf{7c}^{+}$, $\mathbf{7c}^{\cdot-}$) and are reinforcing the observation that tellurium is having a noticeable effect in these systems.

Finally, we turn our attention to the observation that 2,5-diphenyltellurophene (**7d**), when subjected to our standard conditions for generating radical cations (5% H_2SO_4/TFAH) yields the ESR spectrum of $\mathbf{7a}^{+}$ under photolysis, with the precipitation of tellurium.

Barton and co-workers [19] have reported the photolysis of 2-phenyltellurophene in ether, which gives 1-phenylbut-3-en-1-yne with precipitation of tellurium. Through the use of isotopic labelling studies, they were able to propose a mechanism consistent with their observation. Work in our laboratories [20] has shown that 1,4-diphenylbutadiyne when photolysed at 60 °C for 20 min in TFAH containing mercury(II) trifluoroacetate produces an ESR spectrum identical to that of the furan radical cation ($\mathbf{7a}^{+}$), however, when photolysed in our standard solution, 1,4-diphenylbutadiyne did not reveal any trace of $\mathbf{7a}^{+}$. Clearly, the butadiyne is not involved under our conditions.

The formation of **7a** in our case must follow a similar mechanism to that operating when 2-phenyltellurophene is photolysed in ether. Barton's detailed

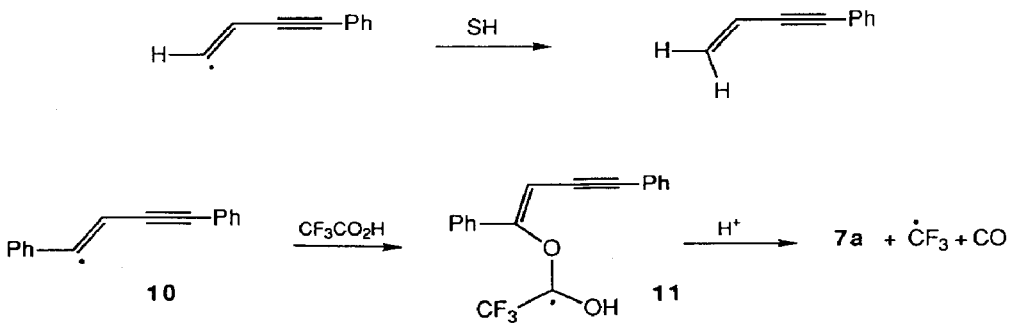

Scheme 1

studies imply that the eventual product in his photolysis arises from a free-radical abstraction of hydrogen from the solvent (Scheme 1).

Invoking a similar intermediate (**10**) in our reaction might lead, in the absence of a suitable hydrogen donor, to free-radical addition to the solvent to give the highly stabilized radical (**11**). The acidic medium might then promote cyclization to give the furan (**7a**). Only minute amounts of **7a** are necessary for the observation of its radical cation ($\mathbf{7a}^{+\cdot}$) by ESR, presumably because **7a** is more readily oxidized in our standard solution than **7d**.

To support the ESR results, we attempted to isolate **7a** from an experiment involving a larger quantity (ca. 20 mg) of **7d**. In an extended photolysis (ca. 8 h), however, there was no indication of the presence of **7a** from NMR spectroscopy, demonstrating how little is required in the ESR study.

Conclusion

The proton hyperfine coupling constants in the ESR spectra of the 2,5-diphenylchalcophene radical catioons ($\mathbf{7a}$–$\mathbf{7c}^{+\cdot}$) are similar for corresponding positions and are consistent with a SOMO which is antisymmetric, with a node through the heteroatom and best represented by **8**.

In the case of the radical anions ($\mathbf{7a}$–$\mathbf{7c}^{-\cdot}$), the observed couplings are affected by the heteroatom, with steady increases in what we believe is the coupling to the heterocyclic protons (H-3) and steady decreases in the coupling to the *para* protons (H-4′), as the atomic weight of the chalcogen is steadily increased. We have argued that these observations are consistent with a SOMO which is symmetric, similar to **9**, with non-zero coefficient on the heteroatom.

The 2,5-diphenyltellurophene radical ions ($\mathbf{7d}^{+\cdot}$, $\mathbf{7d}^{-\cdot}$) show significant increases in coupling to most protons over the other members in the series. In the case of $\mathbf{7d}^{-\cdot}$ we have argued that this is consistent with a SOMO like **9** in which the electropositive heteroatom has a large influence on the spin distribution, while in the case of $\mathbf{7d}^{+\cdot}$ we have suggested that a change in the nature of the SOMO, over that which is operating in the other radical anions, might account for our observations.

Surprisingly, **7d** also undergoes an interesting transformation upon photolysis in H_2SO_4/TFAH, yielding the ESR spectrum of the furan radical cation ($\mathbf{7a}^{+\cdot}$). We have accounted for this observation through a modification of the mechanism proposed by Barton et al.

Experimental

INDO hyperfine coupling calculations [14,21] were performed on the PM3-optimized geometry of 2,5-diphenylfuran. Rotational barriers were calculated with PM3 at the Restricted Hartree–Fock (RHF) level for **7a** and at the Unrestricted Hartree–Fock (UHF) level for $\mathbf{7a}^{\ddagger}$ and $\mathbf{7a}^{\dot{-}}$ using MOPAC Version 5 [22]. All calculations were performed on a VAX 6310 computer.

2,5-Diphenylfuran (**7a**) was purchased from Lancaster Synthesis and purified by chromatography prior to use. 2,5-Diphenylthiophene (**7b**) was prepared by the method of Kumada et al. [23]. 2,5-Diphenylselenophene (**7c**) was prepared by a modification of the method of Lalezari and co-workers [24]. 2,5-Diphenyltellurophene (**7d**) was prepared by a modification of the procedure of Mack [25]. The spectroscopic details of all four chalcophenes are reported below, with experimental details of modified procedures.

^{1}H and ^{13}C NMR spectra were recorded in deuteriochloroform using a Varian VXR-400 or XL-200 spectrometer. Electron ionization mass spectra were obtained on a VG 7070H instrument. ESR spectra were recorded using a Varian E109 spectrometer with the facility for photolysis of samples in the cavity with light from a 500W high-pressure mercury arc provided with neutral density and glass filters.

2,5-Diphenylfuran (7a)

^{1}H NMR: δ 6.75(s, 2H); 7.24–7.46(m, 6H); 7.73–7.79(m, 4H). ^{13}C NMR: δ 107.2; 123.7; 127.3; 128.7; 128.9; 130.8. MS *m/e* 220 (100%, M^{+}); 191(61%); 115(49%); 77(37%).

2,5-Diphenylthiophene (7b)

^{1}H NMR: δ 7.29(s, 2H); 7.28–7.41(m, 6H); 7.61–7.65(m, 4H). ^{13}C NMR: δ 124.0; 125.6; 127.5; 128.9; 134.3; 143.6. MS *m/e* 236 (100%, M^{+}); 202(7%); 121(15%); 77(9%).

2,5-Diphenylselenophene (7c)

Selenium powder (3.16 g, 0.04 mol) and phenylethyne (8.16 g, 0.08 mol) were stirred under reflux for 8 h. After the mixture was cooled, the solid was filtered off and separated by flash chromatography using 5/1 hexane/dichloromethane as eluent, to give a pale solid which was recrystallized from ethanol as silver plates (1.2 g, 11%): m.p. 170–170.5 °C (172 °C [24]). ^{1}H NMR: δ 7.45 (s, 1.86H; d, 0.14H, ^{3}J(H–^{77}Se) 2.9 Hz); 7.24–7.42(m,6H); 7.56–7.61(m,4H). ^{13}C NMR: δ 126.1; 126.2; 127.6; 128.9; 136.3; 149.8. MS *m/e* 284(88%, M^{+}); 203(100%); 202(93%); 102(10%).

2,5-Diphenyltellurophene (7d)

A saturated solution of sodium borohydride in water was slowly added to a stirred suspension of tellurium powder (500 mg, 3.92 mmol) in water (10 ml) heated to 80 °C. During the addition, a steady stream of nitrogen was passed through the solution, which turned purple as the tellurium dissolved. When the solution became colourless, the addition of sodium borohydride was ceased. After the solution was cooled to room temperature, a solution of 1,4-diphenylbutadiyne (800 mg, 3.96 mmol) in hot ethanol (50 ml) was added, followed by heating at reflux for 1 h.

After the mixture was cooled, the solid was filtered off and recrystallized from methanol/chloroform to give **7d** as shiny golden plates. (450 mg, 35%): m.p. 214.5–215 °C. ^{1}H NMR δ 7.84(s, 1.86H; d, 0.14H, ^3J(H–^{125}Te) 5.8 Hz); 7.25–7.37(m, 6H); 7.47–7.51(m, 4H). ^{13}C NMR: δ 126.7; 127.6; 129.0; 133.9; 139.9; 148.2. MS *m/e* 334 (73%, M^+); 203(100%); 149(27%); 102(67%). Anal. Found: C, 57.66; H, 3.33. $C_{14}H_{12}Te$ calcd.: C, 57.91; H, 3.64%.

Acknowledgements

We thank the SERC for financial support and the Ramsay Memorial Fellowships Trust for a fellowship to C.H.S.

References

1 J.L. Courtneidge and A.G. Davies, Acc. Chem. Res., 20 (1987) 90.
2 W. Lau, J.C. Huffman and J.K. Kochi, J. Am. Chem. Soc., 104 (1982) 5515.
3 W. Lau and J.K. Kochi, J. Org. Chem., 51 (1986) 1801.
4 W. Lau and J.K. Kochi, J. Am. Chem. Soc., 108 (1986) 6720.
5 I.H. Elson and J.K. Kochi, J. Am. Chem. Soc., 95 (1973) 5060.
6 W. Lau and J.K. Kochi, J. Am. Chem. Soc., 106 (1984) 7100.
7 D.N.T. Rao and M.C.R. Symons, J. Chem. Soc. Perkin Trans. 2, (1983) 135.
8 M. Shiotani, Y. Nagata, M. Tasaki, J. Sohma and T. Shida, J. Phys. Chem., 87 (1983) 1170.
9 A.G. Davies, L. Julia and S.N. Yazdi, J. Chem. Soc. Perkin Trans. 2, (1989) 239.
10 Landolt–Börnstein, Numerical Data and Fundamental Relationships in Science and Technology, vol. 9, Part d1, Springer-Verlag, West Berlin, 1980.
11 A. Modelli, M. Guerra, D. Jones, G. Distefano and G.C. Pappalardo, Chem. Phys., 88 (1984) 455.
12 G.F. Pedulli, M. Tiecco, M. Guerra, G. Martelli and P. Zanirato, J. Chem. Soc. Perkin Trans. 2, (1978) 212.
13 M. Luisa, T.M.B. Franco, M. Celina, R.L.R. Lazana and B.J. Herold, J. Chem. Soc. Perkin Trans. 2, (1987) 1407.
14 J.A. Pople and D.L. Beveridge, Approximate Molecular Orbital Theory, McGraw-Hill, New York, 1970.
15 J.J.P. Stewart, J. Comput. Chem., 10 (1989) 209.
16 J.J.P. Stewart, J. Comput. Chem., 10 (1989) 221.
17 M.F. Chiu, B.C. Gilbert and P. Hanson, J. Chem. Soc. B, (1970) 1700.
18 A.G. Davies and C.H. Schiesser, unpublished observations.
19 T.J. Barton, C.R. Tully and R.W. Roth, J. Organomet. Chem., 108 (1976) 183.
20 A.G. Davies and P.S. Gregory, unpublished observations.
21 Quantum Chemistry Programme Exchange, QCPE No. 274.
22 Quantum Chemistry Programme Exchange, QCPE No. 455.
23 K. Tamao, S. Kodama, I. Nakajima, M. Kumada, A. Minato and K. Suzuki, Tetrahedron, 38 (1982) 3347.
24 I. Lalezari, A. Shafice, F. Rabet and M. Yalpani, J. Heterocyclic Chem., 10 (1973) 953.
25 W. Mack, Angew. Chem. Int. Ed. Engl., 5 (1966) 896.